

Simulation of the enhanced Curie temperature in $\text{Mn}_5\text{Ge}_3\text{C}_x$ compounds

I. Slipukhina,¹ E. Arras,¹ Ph. Mavropoulos,² and P. Pochet¹

¹*Laboratoire de simulation atomistique (L_Sim),
SP2M, INAC, CEA, 38054 Grenoble cedex 9, France*

²*Institut für Festkörperforschung and Institute for Advanced Simulation,
Forschungszentrum Jülich, D-52425 Jülich, Germany*

(Dated: February 17, 2009)

Abstract

$\text{Mn}_5\text{Ge}_3\text{C}_x$ films with $x \geq 0.5$ were experimentally shown to exhibit a strongly enhanced Curie temperature T_C compared to Mn_5Ge_3 . In this letter we present the results of our first principles calculations within Green's function approach, focusing on the effect of carbon doping on the electronic and magnetic properties of the Mn_5Ge_3 . The calculated exchange coupling constants revealed an enhancement of the ferromagnetic Mn-Mn interactions mediated by carbon. The essentially increased T_C in $\text{Mn}_5\text{Ge}_3\text{C}$ is well reproduced in our Monte Carlo simulations and together with the decrease of the total magnetisation is found to be predominantly of an electronic nature.

Intense efforts have recently been devoted to the fabrication of high- T_C metal/metalloid materials for their potential incorporation into spintronic devices. Among them, Mn_5Ge_3 seems to be a promising candidate due to its compatibility with mainstream silicon technology¹. The low Curie temperature ($T_C = 304 \text{ K}^2$) of this compound, which is a main disadvantage for technological applications, has recently been overcome by carbon doping in $\text{Mn}_5\text{Ge}_3\text{C}_x$ films.³ It was shown³ that carbon incorporation into the octahedral voids of the hexagonal Mn_5Ge_3 cell leads to a continuous increase of T_C with the doping level in $\text{Mn}_5\text{Ge}_3\text{C}_x$ and suggests a saturation when all octahedral voids are filled by carbon. A maximum T_C of 445 K was obtained for $\text{Mn}_5\text{Ge}_3\text{C}_{0.8}$ films, obtained by magnetron sputtering. The carbon implanted $\text{Mn}_5\text{Ge}_3\text{C}_{0.8}$ films were found to exhibit magnetic properties very similar to their sputtered counterparts⁴. The average saturated moment of $2.2 \mu_B/\text{Mn}$ was observed for C-implanted $\text{Mn}_5\text{Ge}_3\text{C}_{0.8}$ films ($1.1 \mu_B/\text{Mn}$ in the sputtered samples) and turned to be somewhat smaller than $2.6 \mu_B/\text{Mn}$ of Mn_5Ge_3 polycrystals⁴. At the same time, the isostructural antiferromagnetic Mn_5Si_3 with $T_N=98 \text{ K}$ was reported to exhibit ferromagnetism when doped with carbon, with the transition temperature reaching 350 K in $\text{Mn}_5\text{Si}_3\text{C}_{0.8}$ ⁵.

While in $\text{Mn}_5\text{Si}_3\text{C}_x$ films the interstitial carbon leads to a lattice expansion, the increase of T_C upon doping in $\text{Mn}_5\text{Ge}_3\text{C}_x$ is accompanied by a lattice compression³. However, it was suggested that the observed lattice distortions in both $\text{Mn}_5\text{Ge}_3\text{C}_x$ and $\text{Mn}_5\text{Si}_3\text{C}_x$ can have a very small influence on the increase of the transition temperatures³. On the other hand, it was also concluded that the double-exchange mechanism plays only a minor role in enhancing the ferromagnetism in $\text{Mn}_5\text{Ge}_3\text{C}_x$. In spite of the existing experimental data on the magnetic properties of C-doped Mn-Ge and Mn-Si compounds, the information about the local magnetic moments, magnetic interactions and the role of carbon interstitials on the enhancement of the T_C of $\text{Mn}_5\text{Ge}_3\text{C}_x$ is still lacking. Hence, in this letter we explore possible zero- and finite-temperature magnetic properties and transition temperatures of the pure and C-doped Mn_5Ge_3 compounds by using first-principles calculations and Monte Carlo simulations.

We follow a standard scheme for the calculation of thermodynamical properties of magnetic systems: (1) first the Green's function formalism and the magnetic force theorem⁶ are employed to determine the exchange integrals J_{ij} from first principles; (2) these are used as input to a classical Heisenberg Hamiltonian of the form $H = -\sum_{i,j;i \neq j} J_{ij} \vec{e}_i \vec{e}_j$, where i and j are the site indexes and \vec{e}_i is a unit vector along a spin moment at i . The T_C is estimated

from the peak in susceptibility-temperature curve, obtained by Monte Carlo simulations using 2160 magnetic-atom supercells. The *ab initio* calculations are performed by the full-potential screened Korringa-Kohn-Rostoker (KKR) Green function method⁷ within the local spin density approximation⁸ of density functional theory. For structural relaxation we use the projector-augmented wave approach as implemented in the ABINIT code,⁹ within the generalized gradient approximation for the exchange-correlation energy.¹⁰

In order to study the effect of structure relaxations on the magnetic properties of Mn_5Ge_3 and $\text{Mn}_5\text{Ge}_3\text{C}_x$, we performed calculations for both *rigid* and *relaxed* lattices. We have used the following lattice parameters for Mn_5Ge_3 , as well as non-relaxed C-doped Mn_5Ge_3 : $a = 7.184 \text{ \AA}$, $c/a = 0.703$ ¹¹. The structure of the $\text{Mn}_5\text{Ge}_3\text{C}_x$ system at $x = 1.0$ was relaxed at the experimentally obtained parameters of $\text{Mn}_5\text{Ge}_3\text{C}_{0.75}$ films³: $a = 7.135 \text{ \AA}$, $c/a = 0.700$. The unit cell of the hexagonal Mn_5Ge_3 (space group $P6_3/mcm$, $D8_8$ -type structure¹¹) contains two sublattices of Mn (Mn_I and Mn_II) with different coordination. The crystalline structure of the $\text{Mn}_5\text{Ge}_3\text{C}_x$ (Fig. 1) was found to be similar to the Mn_5Ge_3 structure with carbon atoms occupying interstitial positions at the center of Mn_II octahedron³.

According to neutron scattering experiments¹², the difference in local environment of Mn_I and Mn_II atoms in Mn_5Ge_3 is believed to be responsible for the different magnetic moments on them. The calculated spin moments on Mn_I , Mn_II and Ge atoms in *relaxed (rigid)* Mn_5Ge_3 are equal to 2.11(2.09), 3.11(3.15) and $-0.14(-0.15) \mu_B$ correspondingly and are almost unaffected by structural relaxation. The smaller magnetic moment on Mn_I is due to a direct Mn_I - Mn_I interaction at a rather short distance (2.526 \AA).¹² The obtained values agree well with the previous calculations^{1,13} and experimental observations¹². The electronic density of states (DOS) (Fig. 2) is metallic, in agreement with the recent calculations.¹ The partial DOS of Mn atoms is dominated by the $3d$ -states, while the largest contribution to Ge DOS is due to $4p$ - and $4s$ - states. The DOS at the Fermi level (E_F) is dominated by the Mn d -states, pointing at the significant Mn-Mn interaction.¹ The exchange splitting is larger for Mn_II d -states compared to Mn_I , in agreement with the larger magnetic moment on Mn_II .

In order to understand the role of C doping in the enhancement of T_C , we first calculated the structurally *non-relaxed* $\text{Mn}_5\text{Ge}_3\text{C}$ unit cell with two carbon atoms in the octahedral voids and compared it to the corresponding results for the undoped compound. Such situation represents the pure hybridization effect between the carbon and the neighboring Mn_II

atoms. As it follows from Fig. 2, carbon incorporation into Mn_5Ge_3 essentially changes the $3d$ -states of Mn_{II} , leaving the corresponding Mn_{I} states almost unaffected. The hybridization between the C $2p$ - and Mn_{II} $3d$ -states leads to a shift of the main occupied peaks in the majority, as well as unoccupied peaks in the minority $3d$ DOS of Mn_{II} towards E_{F} , consequently increasing the density of states $N(E_{\text{F}})$ at the E_{F} in both spin channels. The exchange splitting is now lower than in the pure Mn_5Ge_3 , resulting in a reduced magnetic moment on Mn_{II} . The magnetic moment of the cell is mainly contributed by the Mn_{I} and Mn_{II} atoms ($\mu_{\text{Mn}_{\text{I}}} = 2.21 \mu_{\text{B}}$, $\mu_{\text{Mn}_{\text{II}}} = 2.37 \mu_{\text{B}}$), while the induced magnetic moments on Ge and C ($\mu_{\text{Ge}} = -0.14 \mu_{\text{B}}$, $\mu_{\text{C}} = -0.26 \mu_{\text{B}}$) are much smaller and are antiparallel to the moments on Mn. The structure relaxations caused by interstitial atoms decrease the interatomic Mn-Mn distances (Tab. I), reducing the magnetic moments to $\mu_{\text{Mn}_{\text{I}}} = 1.99 \mu_{\text{B}}$, $\mu_{\text{Mn}_{\text{II}}} = 2.14 \mu_{\text{B}}$, $\mu_{\text{Ge}} = -0.13 \mu_{\text{B}}$ and $\mu_{\text{C}} = -0.21 \mu_{\text{B}}$. However, the effect of hybridization on the decrease of the total magnetisation is much larger than the effect of relaxation. This conclusion follows from our electronic structure calculations for the relaxed $\text{Mn}_5\text{Ge}_3\text{C}$ system with the empty spheres at carbon positions (further referred to as $\text{Mn}_5\text{Ge}_3\text{V}_{\text{C}}$). The calculated magnetic moments on Mn agree well with the average saturated moment of $2.2 \mu_{\text{B}}/\text{Mn}$, observed for the C-implanted $\text{Mn}_5\text{Ge}_3\text{C}_{0.8}$ films,⁴ but deviate from those obtained for the sputtered samples, where the largest moment of $1.1 \mu_{\text{B}}/\text{Mn}$ was observed for $\text{Mn}_5\text{Ge}_3\text{C}_{0.75}$.³ This discrepancy could be ascribed to disorder effects and defects formation, which may differ in sputtered and implanted samples.

In Tab. I we present some of the important calculated exchange constants for the relaxed and rigid Mn_5Ge_3 and $\text{Mn}_5\text{Ge}_3\text{C}$ systems (see Fig. 1 on the notation). Only the interactions between Mn spins are shown, as Mn-Ge interactions turned to be negligibly small. The first nearest neighbor $\text{Mn}_{\text{I}}\text{-Mn}_{\text{I}}$ interactions J_1 (at the shortest distance of 2.526 \AA) are ferromagnetic (FM) and clearly dominate over the corresponding $\text{Mn}_{\text{I}}\text{-Mn}_{\text{II}}$ and $\text{Mn}_{\text{II}}\text{-Mn}_{\text{II}}$ interactions, confirming the assumption about the different magnitude of exchange interaction for Mn atoms in different sublattices¹⁴. The dependence of the exchange parameters on the interatomic distances is stronger for the Mn_{II} sublattice, while it is weaker for the Mn_{I} one. As it follows from Tab. I, there is an antiferromagnetic (AFM) J_3 interaction between the Mn_{II} atoms within $z = \frac{1}{4}$ and $z = \frac{3}{4}$ planes (perpendicular to the c -axis), and FM J_4 and J_6 interactions between Mn_{II} belonging to different planes. The negative sign for J_3 could be responsible for the small degree of non-collinearity in Mn_5Ge_3 , observed in the previous

first-principles calculations¹³. However, an increase of the corresponding Mn_{II}-Mn_{II} distance from 2.974 Å to 3.057 Å after structure relaxation leads to the change from AFM to FM J_3 parameter, while the rest of the parameters are left almost unchanged. As a result the estimated value of the $T_C = 400$ K for the *relaxed* Mn₅Ge₃ system is somewhat higher than for the *rigid* one of 320 K, the latter being in a very good agreement with the corresponding experimentally observed value of 304 K².

The results presented in Tab. I show that interstitial carbon, even without relaxation, significantly changes the value of J_2 , J_3 and J_6 , leaving the J_4 and J_1 interactions almost unaffected. In particular, the J_3 interaction becomes strongly FM compared to the undoped Mn₅Ge₃. According to the DOS of Mn₅Ge₃C in Fig. 2, this increase of the FM interaction can probably be explained by the strong p - d hybridization between Mn_{II} and C states, which enhances the hopping of the $3d$ electrons from the partially occupied d -states of one Mn_{II} atom to a $3d$ orbital of the neighboring Mn_{II}. The J_6 parameter, which in the doped compound corresponds to the 180° Mn_{II}-C-Mn_{II} interaction (*dashed* line on Fig. 1), is essentially lower than the corresponding direct Mn_{II}-Mn_{II} exchange in the parent compound, pointing to the possible superexchange interaction between Mn_{II} via carbon, as predicted by Goodenough-Anderson-Kanamori (GAK) rules.¹⁵ According to these, 90° Mn_{II}-C-Mn_{II} interactions should be FM, which is the case for J_3 and J_4 . In this model interatomic exchange constants are strongly dependent on the orbital overlap, and hence sensitive to changes in the interatomic distances. It should be noted that GAK rules have been successfully applied to explain the first-order FM-to-AFM transition in Mn₃GaC_{1- δ} antiperovskite compounds,¹⁶ in which the local environment of Mn atoms is similar to that in Mn₅Ge₃C.

The transition temperature, calculated using the exchange parameters for the *non-relaxed* C-doped system, is essentially higher ($T_C = 430$ K) than in the undoped compound. This is a direct indication that the strongly enhanced FM stability is not related solely to the variation of the Mn-Mn interatomic distances. To distinguish the effect of relaxations from the electronic structure effect on the enhanced FM interaction in Mn₅Ge₃C, we compared the values of the exchange parameters in the Mn₅Ge₃V_C with those calculated for the parent compound. We can conclude that the essential decrease of the Mn_{II}-Mn_{II} distances due to carbon insertion reduces the FM exchange interaction, and has a particular influence on J_3 making it strongly AFM, thus destabilizing the collinear magnetic structure in Mn₅Ge₃V_C (Tab. I). The relaxation makes J_3 in Mn₅Ge₃C somewhat lower, but still high compared

to that in the pure compound. The J_4 parameter is higher in *relaxed* $\text{Mn}_5\text{Ge}_3\text{C}$, pointing to the 90° FM superexchange, enhanced by the corresponding distance decrease. Although the strong hybridization between Mn $3d$ and C $2p$ orbitals leads to the contraction of the interatomic distances and lowers the longer-distance exchange constants, the FM Mn-Mn interactions prevail in the $\text{Mn}_5\text{Ge}_3\text{C}$, thus giving larger contribution to the T_C than the AFM ones. The calculated $T_C=450$ K is only 20 K larger than in the non-relaxed $\text{Mn}_5\text{Ge}_3\text{C}$, pointing to the small effect of the structural distortions on the T_C increase in Mn_5Ge_3 due to C-doping. The obtained value is in a very good agreement with the maximum value of the experimentally measured T_C of 445 K^{3,4}. To summarize, the present studies clarified that the enhanced FM stability of C-doped Mn_5Ge_3 compounds is attributed to the appearance of the 90° FM superexchange between Mn atoms mediated by carbon, while the structural distortions are found to be a secondary effect.

I.S. acknowledges the CEA nanosciences program and P.M. the ESF SONS, Contract ERAS-CT-2003-980409, for partial funding. The simulations were performed at the CEA supercomputing center (CCRT) and at the Jülich Supercomputing center in the framework of the "High Performance Computing" collaboration between CEA and Helmholtz institutes.

-
- ¹ S. Picozzi, A. Continenza, and A. J. Freeman, *Phys. Rev. B* **70**, 235205 (2004).
- ² Y. Tawara and K. Sato, *J. Phys. Soc. Jpn.* **18**, 773 (1963).
- ³ M. Gajdzik, C. Sürgers, M. T. Kelemen, and H. v. Löhneysen, *J. of Magn. Magn. Mat.* **221**, 248 (2000).
- ⁴ C. Sürgers, K. Potzger, T. Strache, W. Möller, G. Fischer, N. Joshi, and H. v. Löhneysen, *Appl. Phys. Lett.* **93**, 062503 (2008).
- ⁵ C. Sürgers, M. Gajdzik, G. Fischer, H. V. Löhneysen, E. Welter, and K. Attenkofer, *Phys. Rev. B* **68**, 174423 (2003).
- ⁶ A. I. Liechtenstein, M. I. Katsnelson, V. P. Antropov, and V. A. Gubanov, *J. Magn. Magn. Mater.* **67**, 65 (1987).
- ⁷ The SPR-TB-KKR package, H. Ebert and R. Zeller, <http://olymp.cup.uni-muenchen.de/ak/ebert/SPR-TB-KKR>.
- ⁸ S. H. Vosko, L. Wilk, and M. Nusair, *Canad. J. Phys.* **58**, 1200 (1980).
- ⁹ X. Gonze et al., *Comp. Mat. Sci.* **25**, 478 (2002).
- ¹⁰ J. P. Perdew, K. Burke, and M. Ernzerhof, *Phys. Rev. Lett.* **77**, 3865 (1996).
- ¹¹ L. Castelliz, *Mh. Chem.* **84**, 765 (1953).
- ¹² J. B. Forsyth and P. J. Brown, *J. Phys.: Condens. Matter.* **2**, 2713 (1990).
- ¹³ A. Stroppa and M. Peressi, *Phys. Stat. Sol. (a)* **204**, 44 (2006).
- ¹⁴ P. Panissod, A. Qachaou, and G. Kappel, *J. Phys. C: Sol. St. Phys.* **17**, 5799 (1984).
- ¹⁵ J.B. Goodenough, *Magnetism and the Chemical Bond*, New York: Interscience, 1963.
- ¹⁶ L.H. Lewis, D. Yoder, A.R. Moodenbaugh, D.A. Fischer, and M-H. Yu, *J. Phys.: Condens. Matter.* **18**, 1677 (2006).

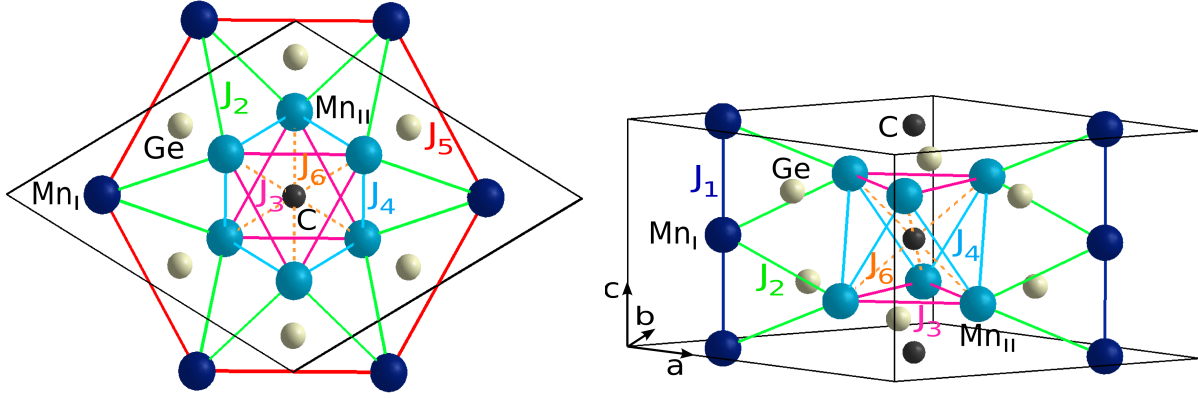


FIG. 1: (Color online) Crystal structure and exchange coupling scheme for the carbon-interstitial phase $\text{Mn}_5\text{Ge}_3\text{C}_x$ at $x = 1$ (full occupancy of carbon): projection on xy -plane (*left*), side view (*right*). Colored spheres denote Ge (grey), Mn_I (dark blue), Mn_{II} (light blue) and interstitial C (black) at the center of Mn_{II} octahedra. Important exchange parameters for different Mn-Mn distances are shown in different colors. The black line indicates the edges of the unit cell.

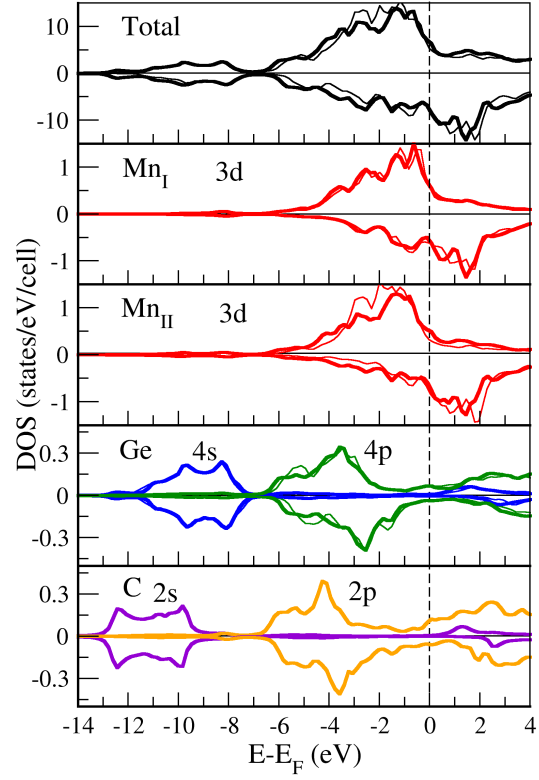


FIG. 2: (Color online) Spin-resolved total and atom-projected DOS, calculated within the KKR method, for the Mn_5Ge_3 (*thin line*) and Mn_5Ge_3C (*thick line*) phases in FM configuration. Note the additional fine structure in the DOS of Mn_{II} for Mn_5Ge_3C due to Mn_{II} -C hybridization.

TABLE I: Calculated (within KKR) exchange constants J_{ij} and T_C for the rigid and relaxed Mn_5Ge_3 and $\text{Mn}_5\text{Ge}_3\text{C}$ compounds. The corresponding Mn-Mn distances (in Å) are shown in square brackets. Positive (negative) values characterize FM (AFM) coupling. Results for $\text{Mn}_5\text{Ge}_3\text{V}_C$ are presented to distinguish between the structural and chemical effects of doping.

J_{ij} (mRy)	Mn_5Ge_3 (rigid)	Mn_5Ge_3 (relaxed)	$\text{Mn}_5\text{Ge}_3\text{C}$ (rigid)	$\text{Mn}_5\text{Ge}_3\text{C}$ (relaxed)	$\text{Mn}_5\text{Ge}_3\text{V}_C$
$J_1^{\text{MnI}-\text{MnI}}$	+2.14 [2.526]	+2.09 [2.527]	+2.24 [2.526]	+2.34 [2.498]	+2.24 [2.498]
$J_2^{\text{MnI}-\text{MnII}}$	+0.59 [3.068]	+0.59 [3.039]	+0.90 [3.068]	+0.69 [3.124]	+0.40 [3.124]
$J_3^{\text{MnII}-\text{MnII}}$	-0.15 [2.974]	+0.13 [3.057]	+0.84 [2.974]	+0.51 [2.714]	-1.80 [2.714]
$J_4^{\text{MnII}-\text{MnII}}$	+0.51 [3.055]	+0.52 [3.082]	+0.44 [3.055]	+0.60 [2.948]	+0.28 [2.948]
$J_5^{\text{MnI}-\text{MnI}}$	-0.10 [4.148]	-0.06 [4.148]	-0.16 [4.148]	-0.22 [4.118]	-0.09 [4.118]
$J_6^{\text{MnII}-\text{MnII}}$	+0.69 [4.263]	+0.65 [4.341]	+0.07 [4.263]	+0.22 [4.008]	+0.76 [4.008]
T_C (K)	320	400	430	450	non-collinear